



The use of cardiovascular magnetic resonance for the assessment of left ventricular hypertrophy

Andrew J. M. Lewis, Oliver J. Rider

Radcliffe Department of Medicine, University of Oxford Centre for Clinical Magnetic Resonance Research (OCMR), University of Oxford, Oxford, UK

Contributions: (I) Conception and design: All authors; (II) Administrative support: All authors; (III) Provision of study materials or patients: All authors; (IV) Collection and assembly of data: All authors; (V) Data analysis and interpretation: All authors; (VI) Manuscript writing: All authors; (VII) Final approval of manuscript: All authors.

Correspondence to: Professor Oliver J. Rider. University of Oxford Centre for Clinical Magnetic Resonance Research (OCMR), Level 0, John Radcliffe Hospital, Oxford OX3 9DU, UK. Email: oliver.rider@cardiov.ox.ac.uk

Abstract: Cardiovascular magnetic resonance (CMR) is a powerful tool to assess and diagnose the cause of left ventricular hypertrophy (LVH). This review provides an overview of the typical CMR findings in the various causes of LVH, focusing mainly on late gadolinium enhancement (LGE) imaging. It will also cover the more novel techniques of T1 mapping, extracellular volume (ECV) fraction estimation and diffusion tensor imaging (DTI) and their role in the imaging assessment of LVH.

Keywords: Left ventricular hypertrophy (LVH); cardiac magnetic resonance (CMR)

Submitted Jan 10, 2020. Accepted for publication Jan 30, 2020.

doi: 10.21037/cdt.2020.01.14

View this article at: <http://dx.doi.org/10.21037/cdt.2020.01.14>

Introduction

In daily clinical practice, cardiologists frequently encounter patients with left ventricular hypertrophy (LVH) of initially unknown origin. The differentiation of either “pathological” hypertrophy (hypertensive heart disease, hypertrophic cardiomyopathy (HCM), myocardial storage/infiltrative disease and others), or “physiological” hypertrophy (athletic training) is key to further management and prognostication. Whilst it is beyond question that the clinical and family history as well as the physical examination (to determine exercise level, history of hypertension, family history of cardiomyopathy and sudden cardiac death among other key factors) will narrow the differential diagnosis, the precise aetiology of LV hypertrophy frequently remains unclear from these steps. In addition, in the context of an obesity epidemic the use of electrocardiography (ECG) and echocardiography for the detection of LVH has become more challenging for the assessment of LVH in many affected patients (1). As a result, cardiovascular magnetic resonance (CMR), which has excellent reproducibility, an

unrestricted field of view and provides non-invasive tissue characterization without ionizing radiation (irrespective of chest wall fat (2) has become a key tool for the early diagnosis and treatment assessment of LVH.

Current barriers to the wider uptake of CMR for the assessment of LVH include relatively long examination times (typically 30–45 minutes), time consuming post-processing, a lack of availability and expertise, and high costs with reimbursement issues in some healthcare systems. In addition, it may not be possible to scan patients with metallic surgical clips, or MR non conditional implantable cardiac electronic devices (CIED) for safety. As a result, CMR tends not to be used as a screening test for LVH, though guidelines from both the European Society of Cardiology (ESC) and American College of Cardiology (ACC) both recommend CMR as a second line test, either when additional diagnostic information is needed if echocardiographic image quality is poor, or when diagnostic uncertainty remains with respect to the diagnosis of HCM (3,4). New accelerated imaging technologies may overcome

some of these barriers.

CMR cine imaging provides a detailed assessment of cardiac morphology and right and left ventricular systolic function with high temporal and spatial resolution, whilst other sequences and contrast techniques allow myocardial tissue characterisation. Whilst the detection of hypertrophy (usually defined as a left ventricular wall thickness >13 mm) immediately opens a differential diagnosis encompassing (amongst many more); hypertension; HCM, sarcoidosis, amyloidosis, Anderson-Fabry disease, mitochondrial disorders and athletic adaptation, in itself the detection of wall thickening does not usually definitively establish the diagnosis. Although there are classical features that point to a diagnosis in many cases from transthoracic ultrasound (speckled myocardium of amyloidosis, asymmetrical septal hypertrophy and LVOT obstruction in HCM) these are not always sensitive or specific, and can be either absent in disease, or a manifestation of a “phenocopy.” *Figure 1* demonstrates five hypertrophied hearts which, by left ventricular geometry alone, cannot be easily separated, but reflect 5 different underlying diagnoses which can be separated according to their distinctive patterns of late gadolinium enhancement (LGE).

This review will describe the situations in which CMR has improved the reliability of LVH diagnosis, focusing mainly on LGE but also highlighting where novel techniques such as native parametric mapping techniques, extracellular volume (ECV) fraction estimation and diffusion tensor imaging (DTI) are enabling further insights into the biology and consequences of diseases causing LVH.

Cardiac amyloidosis

Amyloidosis is a condition characterized by extracellular deposition of pathologic insoluble fibrillar proteins. Cardiac light chain amyloid (AL) amyloidosis, in which amyloid fibrils are derived from monoclonal immunoglobulin light chains, is associated with poor prognosis, with a median untreated survival from diagnosis of <12 months. Transthyretin (TTR) is a plasma protein, predominantly synthesized in the liver, which acts as a transporter for thyroxine and retinol-binding protein. TTR amyloid cardiomyopathy can occur either as a result of deposition of wild type transthyretin protein (ATTRwt) or as an autosomal dominant trait caused by pathogenic mutations in the TTR gene (hATTR, also known as mTTR). The prognosis of transthyretin-related amyloid cardiomyopathy is generally better than that of AL amyloid, though survival

may still only be 3 to 5 years without treatment (5).

Although a rare disease, cardiac amyloidosis is a relatively common cause of ventricular hypertrophy, particularly in older patients. Diagnosis of cardiac amyloidosis is not always straightforward as there are several myocardial disorders that phenocopy cardiac amyloidosis and CMR has quickly become adopted as an imaging technique to clarify diagnosis. The power of CMR for the diagnosis of amyloidosis is based upon the differences in gadolinium wash-out kinetics between myocardium with amyloid deposition and normal myocardium (6). Typical CMR LGE findings include enhancement of both the RV and LV endocardium (giving rise to the so-called “Zebra sign”) and a generally high myocardial signal. This leads to a dark blood pool and difficulty in ‘nulling’ the myocardial signal on phase sensitive inversion recovery sequences. In addition, the pattern and extent of LGE as assessed by CMR appears to provide incremental prognostic value in cardiac amyloidosis: a recent meta-analysis showed that LGE presence on CMR was associated with an increased risk of all-cause mortality in patients with systemic amyloidosis and known or suspected cardiac amyloidosis (7). However, although initial data reported that a transmural LGE pattern was also able to differentiate ATTR from AL cardiac amyloidosis with good accuracy (8) a recent, larger systemic review and meta-analysis did not confirm this. Overall, although CMR is a valuable tool for diagnosing cardiac amyloidosis (sensitivity 85.7%, specificity 92.0% when compared to endo-myocardial biopsy) it is not reliable in further classification of amyloid subtype (9). Additional tests including nuclear scintigraphy, serum and urinary immunofixation and tissue biopsy may all be required. Nuclear scintigraphy using ^{99m}Tc DPD or ^{99m}Tc PYP in contrast to CMR appears to be a powerful tool for differentiating ATTR from AL amyloidosis with meta-analysis showing sensitivity from 90.9% to 91.5% and specificity from 88.6% to 97.1% (9), suggesting it has benefit when incorporated into clinical practice.

Figure 2 shows the typical pattern of LGE seen with cardiac amyloid involvement. The blood-pool is commonly dark in appearance and typical findings would be global, subendocardial LGE. However, it should be noted that LGE-CMR has multiple patterns in amyloidosis in addition to this classical pattern. The pattern of LGE can be atypical and patchy, especially in early disease (10).

Accurate diagnosis and subtyping of cardiac amyloid cardiomyopathy have recently assumed even greater importance following the demonstration of efficacy of

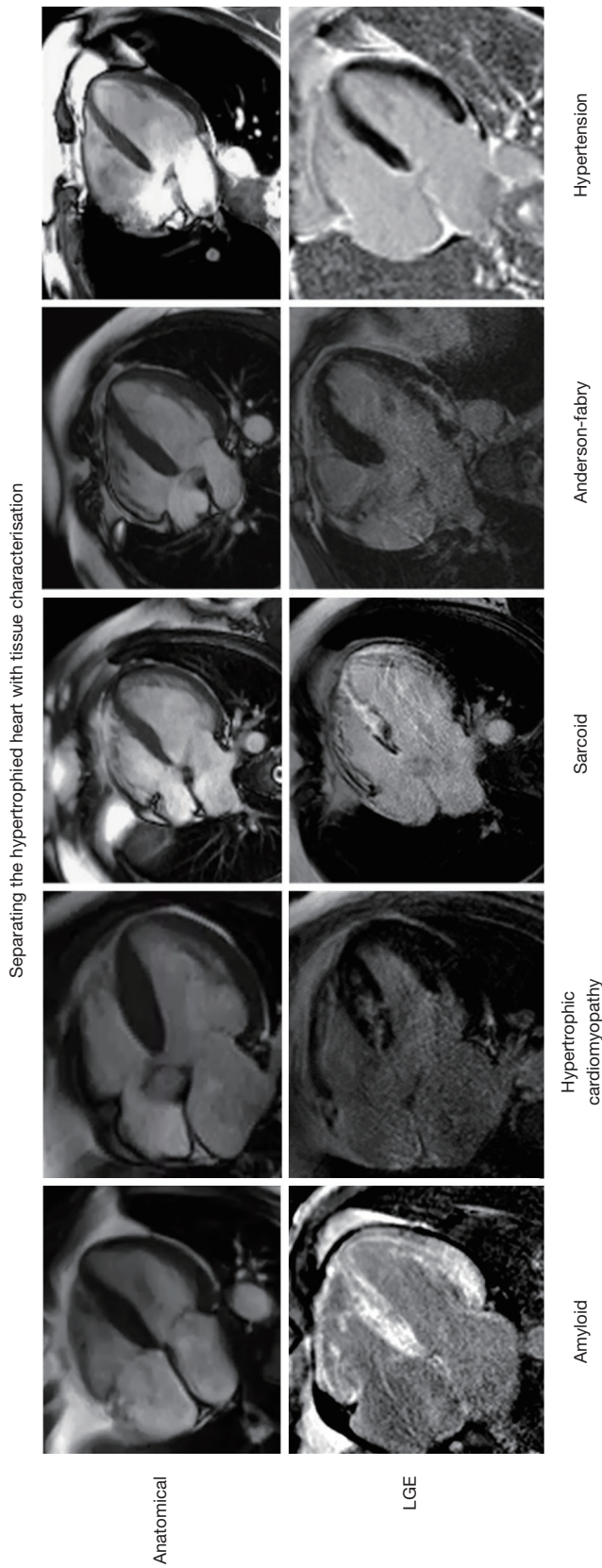


Figure 1 Upper row: 5 CMR horizontal long axis (anatomical) views of 5 hypertrophied hearts with similar phenotype, but differing diagnoses (left to right) amyloid, hypertrophic cardiomyopathy, sarcoid, Anderson-Fabry disease, and hypertensive heart disease. The lower row highlights the late gadolinium findings that allow separation of these diseases. CMR, cardiovascular magnetic resonance.

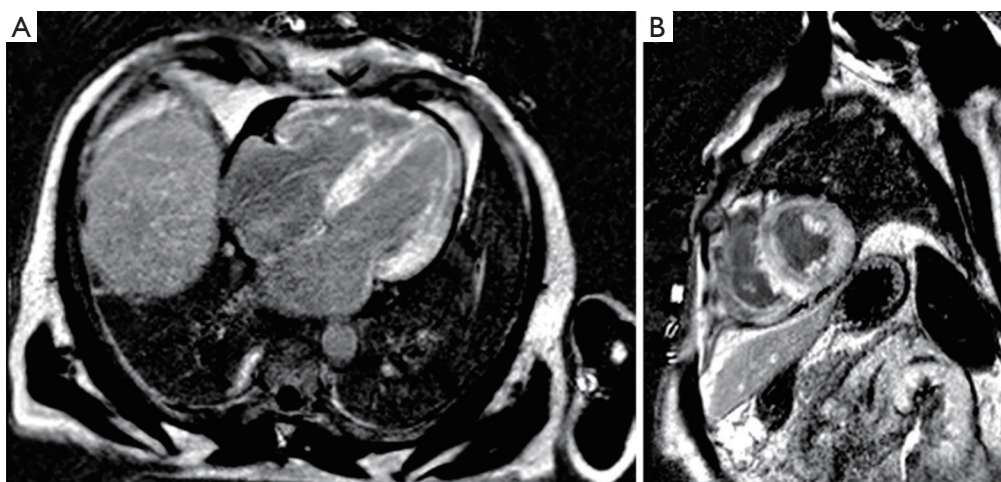


Figure 2 Classical LGE pattern of amyloid involvement in (A) horizontal long axis view and (B) short axis view, showing global sub-endocardial involvement including both sides of the ventricular septum producing a “Zebra” sign appearance. LGE, late gadolinium enhancement.

novel disease modifying agents. New treatments for ATTR amyloid cardiomyopathy include the TTR binding agent tafamidis, which has been shown to improve mortality in cardiac ATTR amyloidosis (hazard ratio for all-cause mortality 0.70, 95% CI, 0.51–0.96) (11). Novel targeted treatments for hATTR amyloidosis including patisiran (12,13) and inotersen (14) have also demonstrated excellent efficacy. Treatment for AL amyloidosis includes chemotherapy and/or novel therapies targeting the underlying plasma cell dyscrasia.

Novel CMR techniques for cardiac amyloidosis

Parametric mapping techniques including native T_1 mapping and extracellular volume (ECV) fraction estimation may offer improved sensitivity to early amyloid disease detection compared to LGE. T_1 represents the time taken for 63% of longitudinal magnetisation to recover after preparation by an inversion recovery radiofrequency pulse and is intrinsically determined by the tissue composition. Body tissues or substances with high water content (e.g., blood or cerebrospinal fluid) have a relatively long T_1 value whereas fat has a relatively short T_1 time, as does any organ with high iron content. When considering myocardial T_1 values, amyloidosis is associated with markedly prolonged native T_1 values (15), which may be patchy in distribution (Figure 3). The underlying mechanisms behind this prolongation in myocardial native T_1 time are incompletely understood but are likely to include the deposition of

amyloid protein, myocardial oedema and interactions between the protein and local water content.

Since amyloidosis is characterised by extracellular deposition of amyloid proteins, quantification of the left ventricular ECV fraction may provide a quantitative, non-invasive assessment of amyloid burden in the heart. ECV fraction is estimated from the concentration of contrast agent in the myocardium relative to blood in a dynamic steady state using post gadolinium T_1 mapping (Figure 4). Although an elevation of cardiac ECV is seen in numerous disease processes, cardiac amyloidosis is associated with the highest ECV of all cardiac diseases, and has been proposed to be a non-invasive marker of disease burden (16). Hence through a combination of native T_1 and ECV mapping it has become possible to improve the diagnostic performance of CMR in cohort studies (Figure 5). Despite this potential, clinical trial data, formalised trials of diagnostic capability, and standardisation remain lacking. LGE techniques remain central to the diagnosis of cardiac amyloidosis using CMR.

HCM

HCM is a common inherited heart muscle disease and is defined as the presence of LVH in the absence of other causes of LVH including abnormal loading conditions (aortic stenosis, arterial hypertension). The prevalence of HCM in the general population is estimated to be approximately 1:500. Given that both hypertension and HCM are common, discriminating the two from each other is a

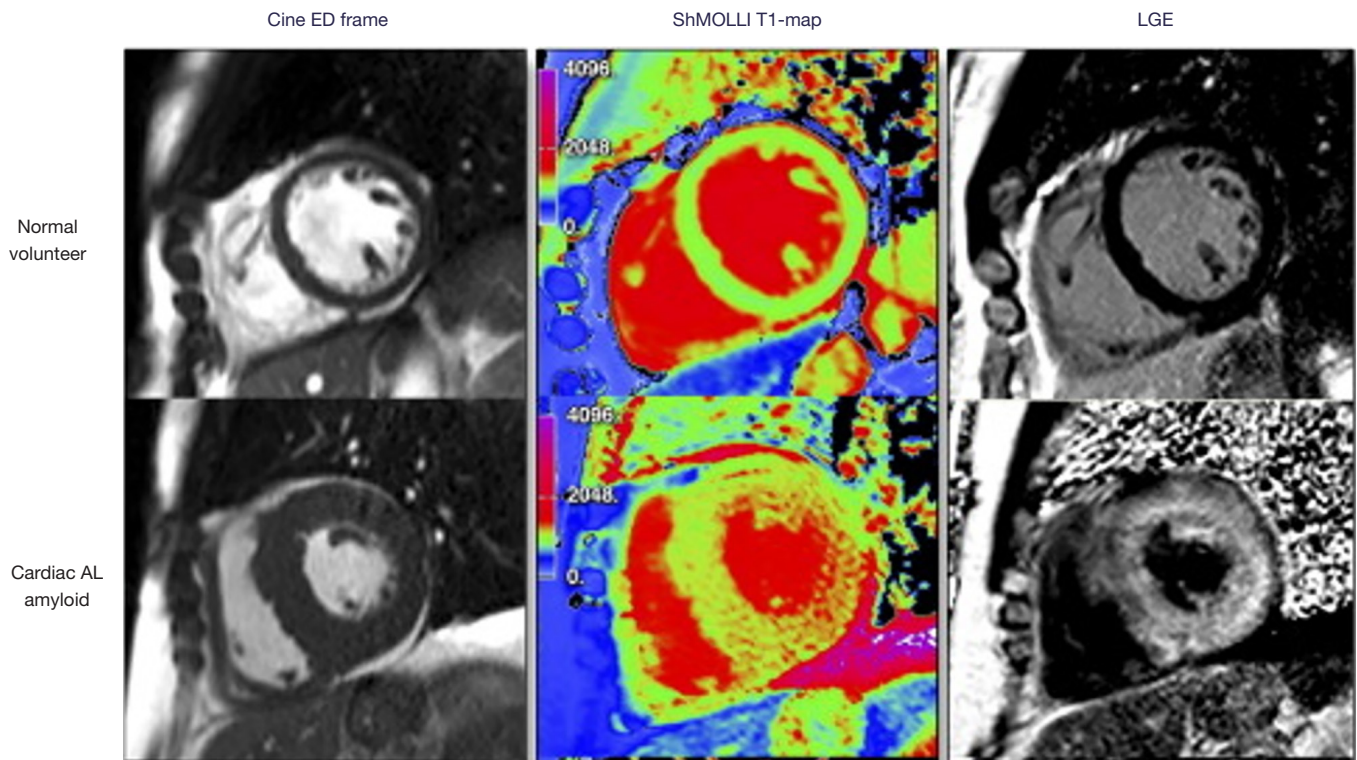


Figure 3 End-diastolic frame from cine (left panel), ShMOLLI T1 map (middle panel), and LGE images (right panel) in normal volunteer, and cardiac amyloid patient showing elevated myocardial T1 time in amyloid (into the red range of the colour scale) compared to the normal control. LGE, late gadolinium enhancement.

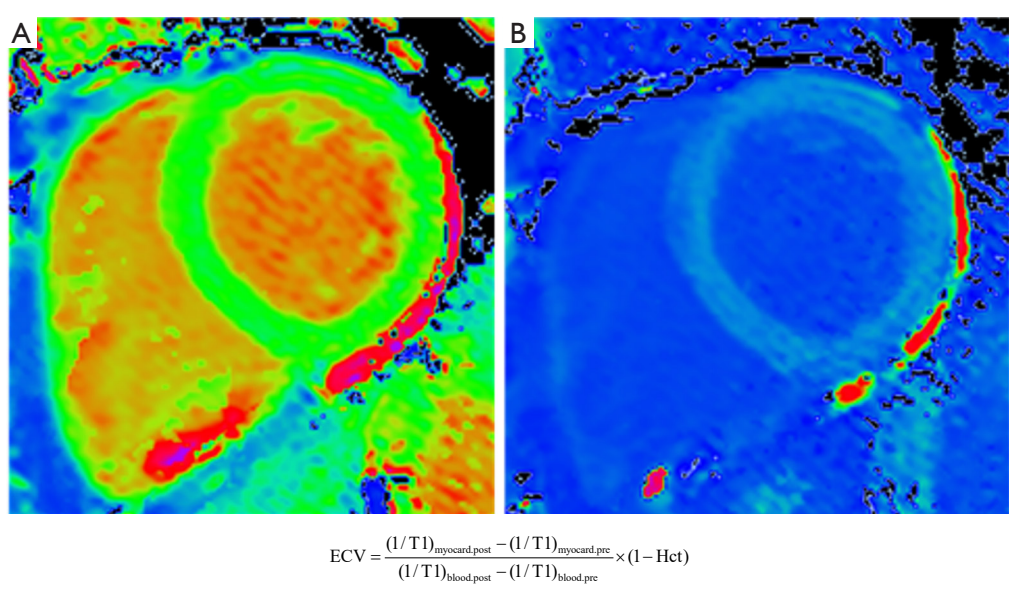


Figure 4 Post gadolinium equilibrium CMR for the calculation of extracellular volume.

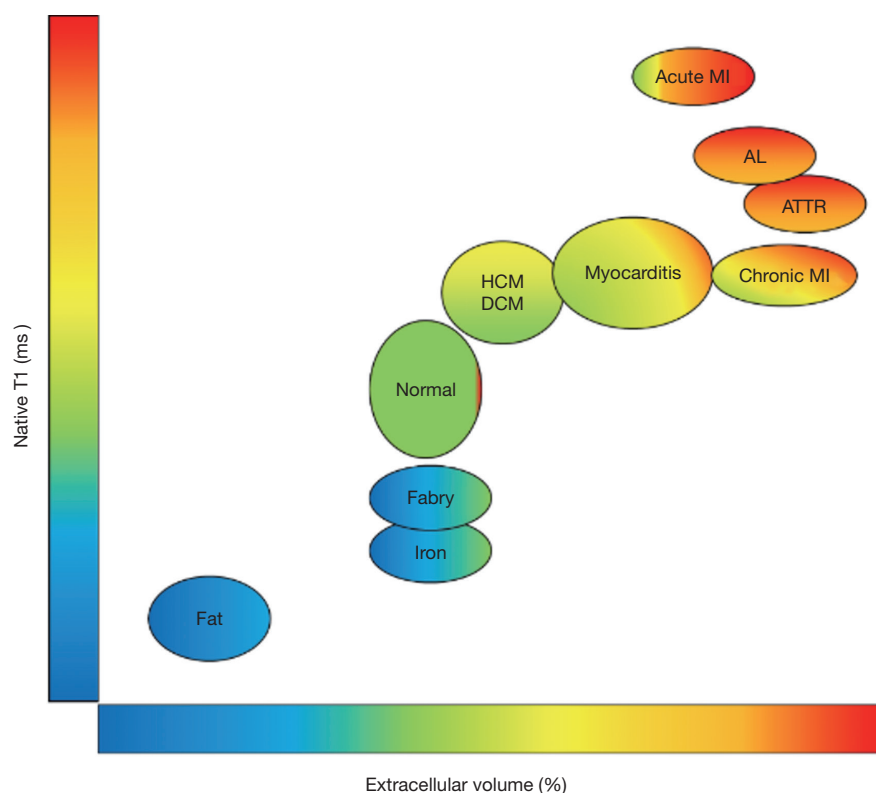


Figure 5 Theoretical disease separation by tissue characterisation using native T1 and post gadolinium ECV. Absolute values for native T1 are variable depending on field strength (1.5 T or 3 T), pulse sequence (MOLLI, ShMOLLI, SASHA), and scanner manufacturer. For the purpose of comparability, no absolute values have been used. ECV, extracellular volume fraction.

common clinical problem, particularly in milder phenotypes of hypertrophy. A careful family history may reveal clues to familial HCM (usually autosomal dominant inheritance caused predominantly by mutations in genes which encode for sarcomeric proteins). The ability of CMR to display the histopathological features of cardiomyocyte hypertrophy, interstitial fibrosis, and more recently myofibrillary disarray make it a useful clinical tool in this setting. As a result, current ESC guidelines suggest a CMR in the absence of contraindications. CMR with LGE is a class I recommendation in patients with suspected HCM who have inadequate echocardiographic windows, in order to confirm the diagnosis, and a class IIa indication to both assess cardiac anatomy, ventricular function, and the presence and extend of fibrosis in those fulfilling criteria, and if apical HCM is suspected (3). Differentiation of early or milder phenotypes of HCM from athletically trained hearts or longstanding hypertension can remain challenging in some situations. This has been separately reviewed elsewhere (17) and whilst imaging can be extremely valuable, other factors

including the 12 lead ECG and the response to a period of athletic detraining may also be needed.

Pattern of hypertrophy in HCM

CMR provides three-dimensional tomographic cardiac imaging with high spatial and temporal resolution in any plane, leading to advantages over transthoracic echocardiography for the assessment of the apex of the heart (which may be challenging in patients with suboptimal acoustic windows) and in imaging discrete areas of hypertrophy that can be easily missed with 2D ultrasound imaging. *Figure 6* shows some of the classical hypertrophy patterns seen with CMR.

In addition to this the presence and pattern of LGE is also helpful in the diagnosis and risk stratification of HCM. There have been several studies describing the distribution of LGE in familial HCM patients and its prognostic value. It is generally accepted that the presence of LGE is predominantly observed at the insertion points of the

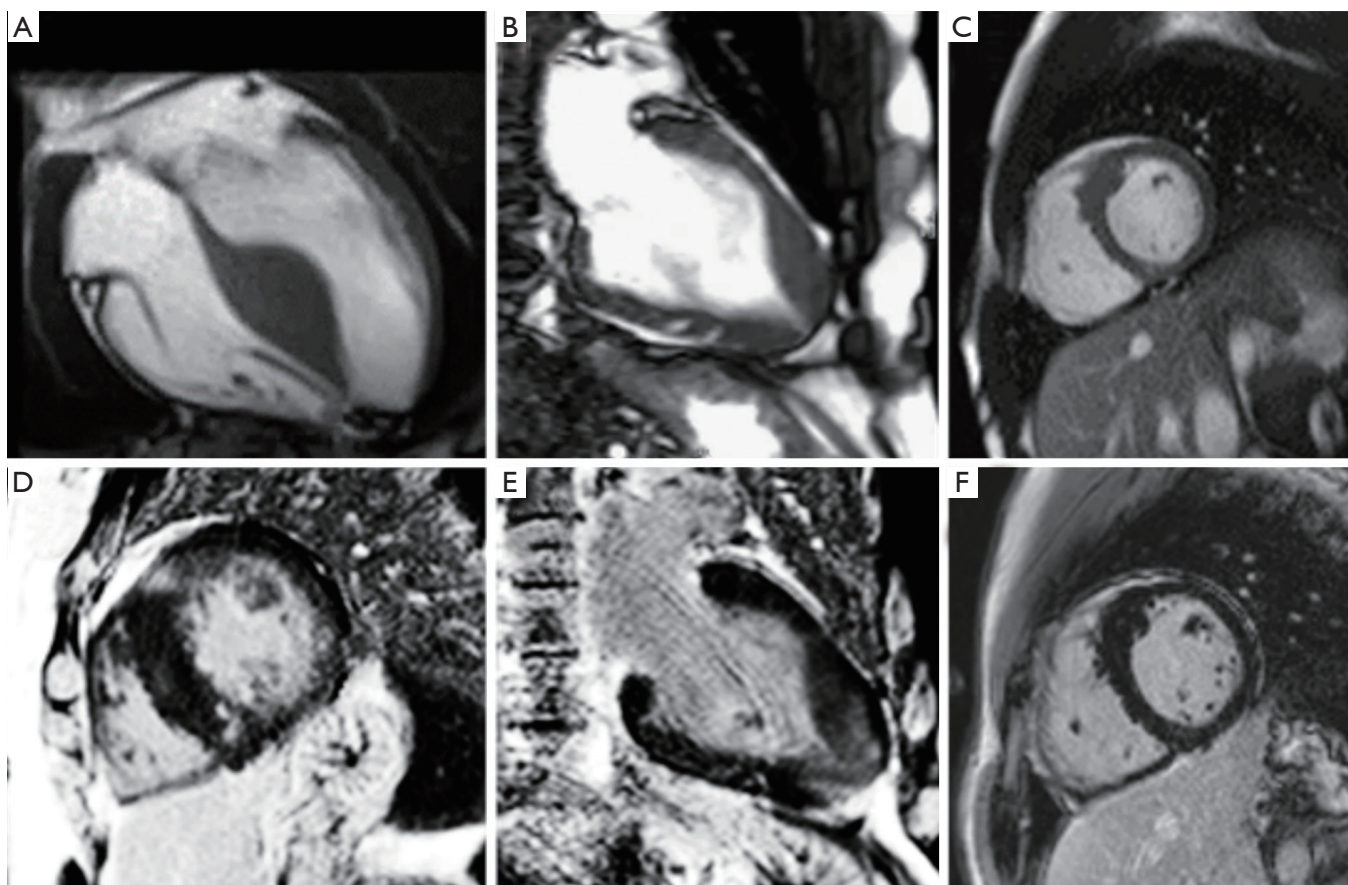


Figure 6 The ability of CMR to show not only the different patterns of hypertrophic cardiomyopathy, (A) classical asymmetrical septal hypertrophy, (B) apical hypertrophy, (C) localised/discreet hypertrophy, but also the differing patterns of fibrosis (D) classical inferior and superior LV/RV junctions and region of hypertrophy, (E) apical fibrosis, (F) fibrosis in the hypertrophied section (in this case minor).

right ventricle into the left ventricle and in the regions of hypertrophy. Although there currently remains some debate as to whether the presence or extent of LGE is prognostic in HCM (the HCMR registry is aimed at investigating this in a large registry) (18) the majority of retrospective cohort studies show that LGE is predictive (and maybe incrementally better than HCM risk-SCD score) of cardiovascular events (19).

T₁ mapping and HCM

As with cardiac amyloidosis, a large amount of research has been performed in T₁ mapping and ECV mapping for the diagnosis and assessment of HCM. An example is the study by Hinojar *et al.*, where native T₁ mapping and ECV fraction were successful on a group level in separating clear cut HCM (average 19±4 mm, and >15 mm wall thickness)

from normal hearts (wall thickness 8±11 mm), and from hypertensive heart disease (14±5 mm). Despite the clear potential, there remains considerable overlap in both native T₁ and ECV values (15,20) between, making the use of T₁ and ECV mapping currently limited to group studies and not reliable on a single patient basis (*Figure 7*). In addition, future studies are also needed to investigate the diagnostic performance of these mapping techniques in clinical situations where the diagnoses are less clear cut, and changes less likely to be pronounced.

Diffusion tensor mapping and HCM

One important recent advance in CMR for the diagnosis and risk stratification of HCM is the development and clinical cardiac application of DTI. It is likely that myocyte disarray is a key pathological substrate for potentially

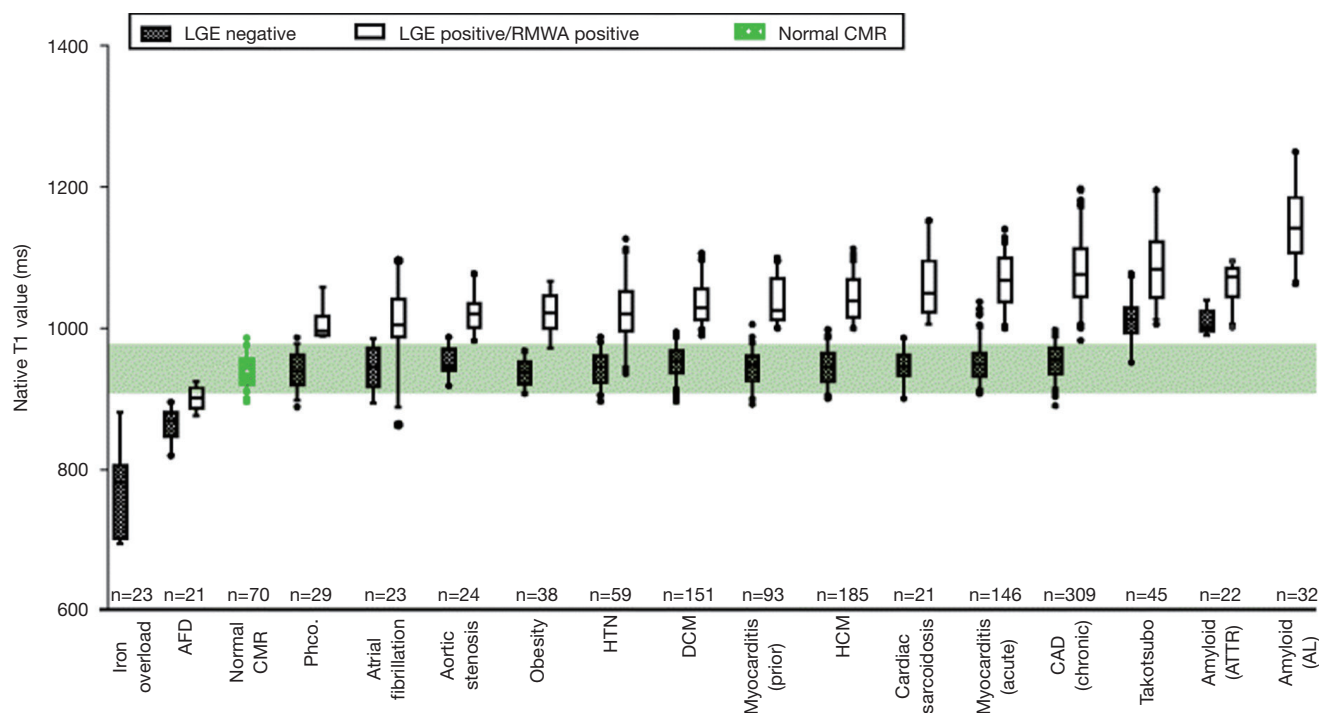


Figure 7 Highlighting the cross over native T1 values in hypertrophy in HCM, Hypertension and Aortic Stenosis, reproduced with permission and without changes under Creative Commons license, from Liu *et al.* (15). HCM, hypertrophic cardiomyopathy.

fatal arrhythmia in HCM although LGE and parametric mapping techniques are not capable of directly assessing this. DTI is capable of assessing the orientation of fibres within an organ by mapping the diffusion of water molecules.

Figure 8 shows how diffusion tensor CMR maps the diffusion of water molecules in three dimensions. Fractional anisotropy (FA) is calculated from the diffusion tensor, quantifying the directionality of water diffusion. In the absence of cellular or intracellular barriers, water motion in the heart would be random and equal in all directions, and as such would have no directionality (i.e., depicted as a sphere using the diffusion tensor) and FA would be zero (perfect isotropy). Cell membranes act as barriers which restrict water motion along the long axis of myocytes. As a result, in HCM FA is expected to be high in areas with coherently aligned myocytes with a consistent orientation. Conversely, FA is expected to be low in voxels with differing myocyte orientations and in HCM due to disorganized cell orientations and expanded ECV. As a result, in a recent study, FA was reduced in HCM and provided arrhythmia risk stratification even correcting for conventional imaging risk factors (21) (Figure 9).

Cardiac sarcoidosis

The prevalence of sarcoidosis is reported to be 10–40/100,000 persons in the United States and Europe (22). Sarcoidosis is commonly reported to affect the lungs, lymph nodes, skin, eyes, and central nervous system. There is however a discrepancy between the number of clinical cases diagnosed with cardiac involvement (~5%), and actual cardiac involvement on autopsy (~25%) (23). Indeed, using advanced imaging, up to ~50% can be shown to have cardiac involvement depending upon the imaging modality used, and the population studied (24).

The cardiac features of sarcoidosis include three successive histological stages: oedema, granulomatous inflammation, and fibrosis leading to post-inflammatory scarring. Sarcoid non-caseating granulomas can involve any part of the heart, although the left ventricle is the most common site.

CMR appears to also be well suited to imaging in sarcoid as it can quantify oedema and fibrosis. No specific pattern of LGE is pathognomonic for cardiac sarcoidosis and images are interpreted in the context of the patient's history and by a cardiologist or radiologist with specific expertise. Whilst

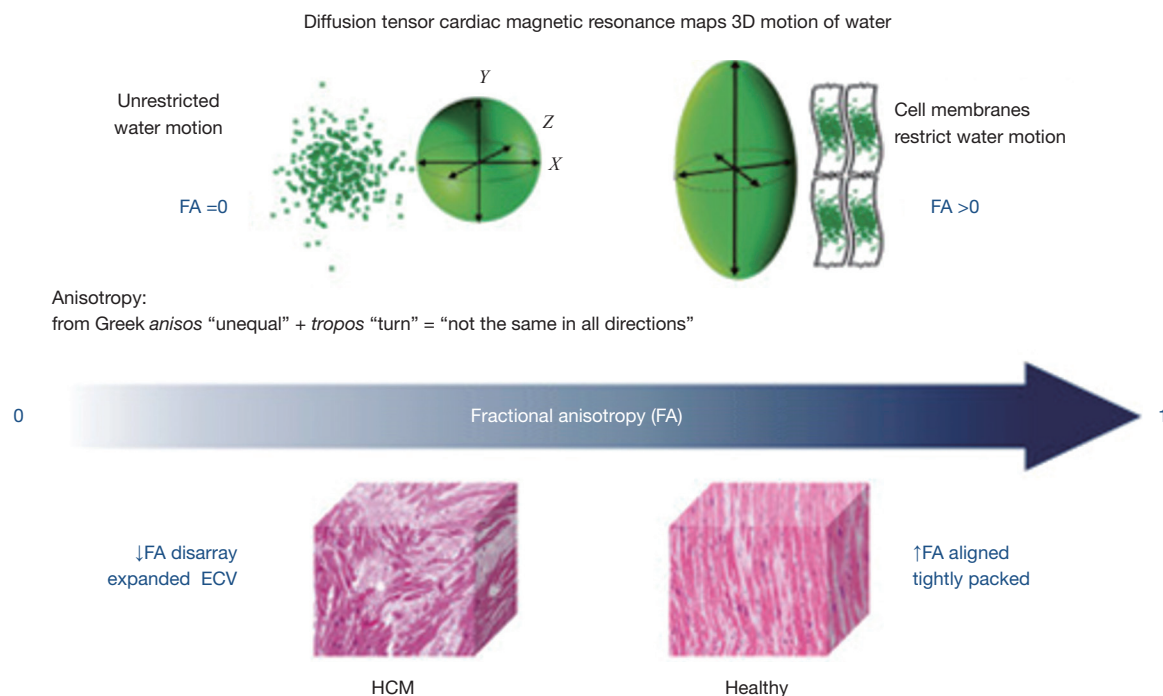


Figure 8 Principles of diffusion tensor imaging for the assessment of myocyte disarray in hypertrophic cardiomyopathy. Reproduced with permission and without changes under Creative Commons license from Ariga *et al.* (21).

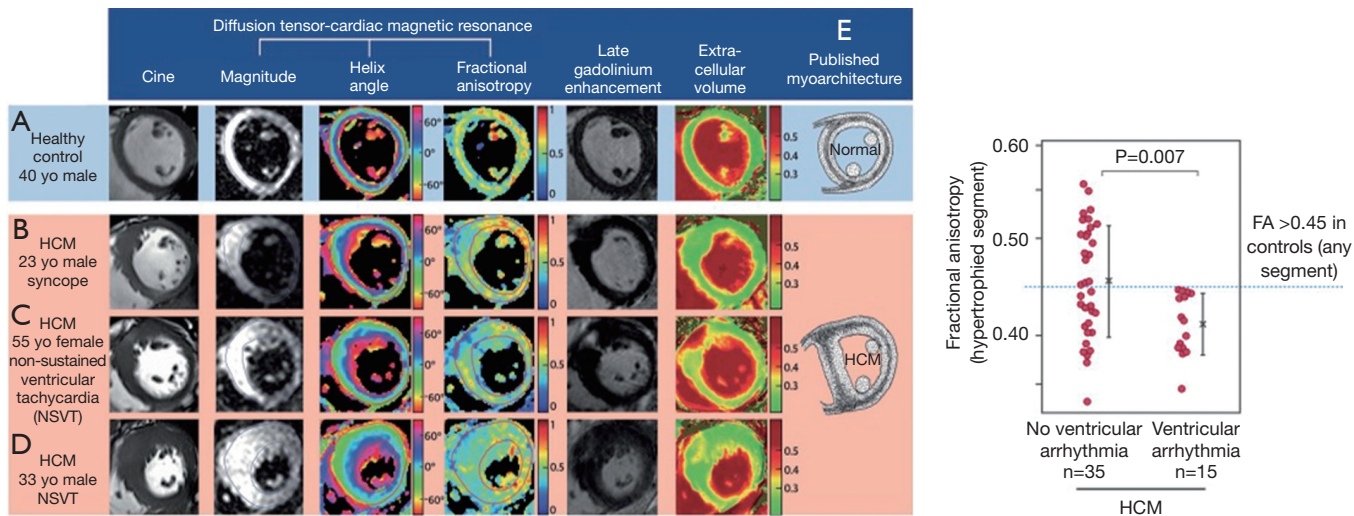


Figure 9 Left panel: DTI-CMR can provide *in vivo* assessment of left ventricular myoarchitecture. The HA is the average myocyte orientation, and FA is a surrogate measure of underlying cell organization. The mid-ventricular slice at diastole in healthy control subjects (A) and patients with HCM (B,C,D) demonstrated similar HA distributions but marked differences in FA. These patterns were consistent with previously published HCM histology that shows disarray and fibrosis invading the mid-wall at the insertion point and hypertrophied segments (E); right panel: diastolic FA, measured in the hypertrophied segment, was reduced in HCM with ventricular arrhythmia compared with those without. Reproduced with permission and without changes under Creative Commons license from Ariga *et al.* (21). HA, helix angle; FA, fractional anisotropy.

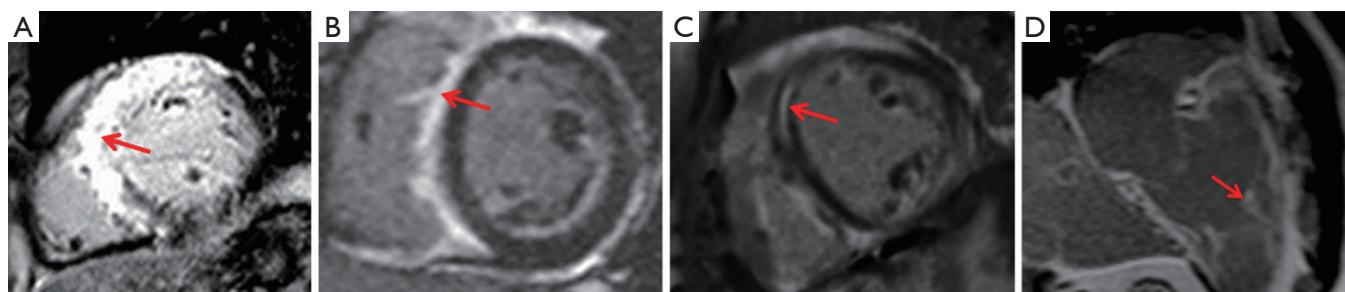


Figure 10 Examples of various patterns of LGE (arrows) seen in cardiac sarcoid (A) transmural, (B) right ventricular endocardial side of the LV septum, (C) mid and sub-epicardial patches, (D) right ventricular involvement.

the most commonly described pattern is one or more patchy regions of LGE that would not be typical for myocardial infarction (sparing the endocardium and not in a coronary territory). However, many other patterns of LGE and even a pattern that is typical for prior myocardial infarction can also represent cardiac sarcoid (*Figure 10*). Current expert consensus for the diagnosis of cardiac sarcoid includes LGE on CMR (in a pattern consistent with CS) (24,25).

Quantitative myocardial tissue characterization with T_1 and T_2 mapping may also enable non-invasive recognition of cardiac involvement and activity of myocardial inflammation in patients with systemic sarcoidosis, by detecting oedema (26).

^{18}F -fluorodeoxyglucose positron emission tomography (^{18}F -FDG PET) provides complementary information to CMR for the assessment of sarcoidosis (27,28) (*Figure 11*). By detecting metabolic activity from activated innate immune cells, ^{18}F -FDG PET allows assessment of disease activity, potentially differentiating active from quiescent sarcoidosis which can be used to guide clinical management (28). In contrast, although CMR LGE has excellent negative predictive value for cardiac sarcoidosis, current CMR techniques cannot separate active from quiescent inflammation, though newer techniques with potential to do this are in development (29,30). Hybrid MR-PET systems can combine high spatial resolution morphological and functional assessment using CMR with ^{18}F -FDG-PET (31). Overall, CMR/PET imaging holds promise for the diagnosis of active cardiac sarcoidosis, providing incremental information about both the pattern of injury and disease activity within a single scan.

Anderson-Fabry disease

X-linked mutations in the α -galactosidase gene cause

Anderson-Fabry disease (AFD). This deficiency results in intracellular accumulation of neutral glycosphingolipids and progressive renal, cardiac, and cerebrovascular disease. Female carriers are at risk of developing disease, but this tends to be milder and more slowly progressive than in males. Cardiac manifestations are typically of a HCM phenocopy, with left ventricular hypertrophy being the most common cardiac manifestation (followed by conduction system disease, valve dysfunction, and arrhythmias). The treatment relies on enzyme replacement therapy and cardiac device therapy for arrhythmias.

CMR is an excellent technique to non-invasively diagnose cardiac involvement in AFD. The major advantage it brings is separating AFD from potential causes of hypertrophy and re-classifying those labelled a diagnosis of HCM. The classical CMR features of AFD are concentric hypertrophy and inferolateral and mid- myocardial scar on LGE imaging (*Figure 12*).

In addition to the late gadolinium imaging native T_1 mapping has been shown to be a useful measure in patients with Anderson-Fabry disease. Given the deposition of sphingolipids, the T_1 values are usually significantly lower in AFD, compared to other causes of LV hypertrophy (32). T_1 values showed pseudonormalization or elevation in the left ventricular inferolateral wall, correlating with the presence or absence of LGE (*Figure 13*).

Cardiac hypertrophy due to pressure overload

Hypertensive heart disease and aortic stenosis are both common causes of ventricular hypertrophy due to pressure loading. Whilst the cause of both is usually apparent at the diagnosis of LVH, CMR is sometimes sought to exclude another pathology, such as amyloidosis. This extends to obesity (34,35), where LVH is seen, and echo based techniques

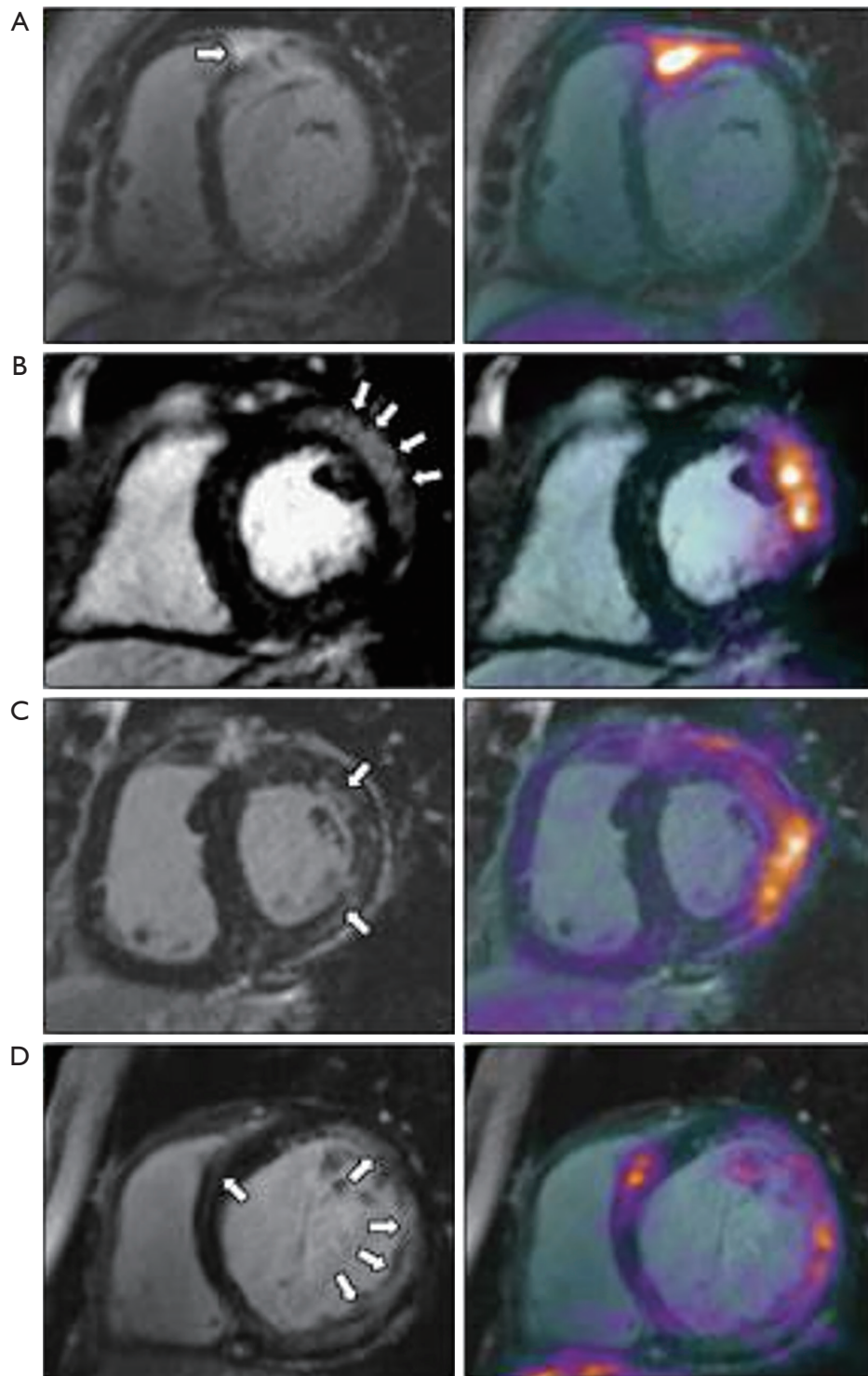


Figure 11 Imaging active cardiac sarcoidosis. Reproduced from Dweck *et al.* (28). Left panel: LGE MRI. Right panel: hybrid LGE and ^{18}F -FDG. (A) Subepicardial LGE in basal anteroseptum extending into right ventricular free wall and increased ^{18}F -FDG uptake at same region on fused PET-MR; (B) subepicardial LGE (arrows) in the basal anterolateral wall with increased ^{18}F -FDG uptake co-localizing to identical region on PET-MR; (C) patchy midwall LGE (arrows) in anterolateral wall with matched increased ^{18}F -FDG uptake on PET-MR; (D) multifocal LGE (arrows) in lateral wall with matched increased ^{18}F -FDG uptake on PET-MR. LGE, late gadolinium enhancement.

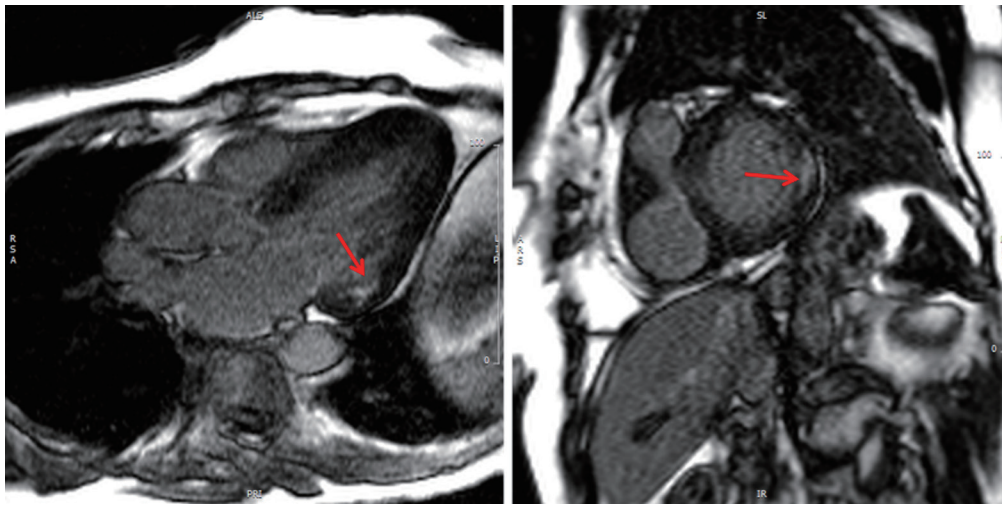


Figure 12 Mid-wall fibrosis (arrows) in the basal inferior lateral wall in Anderson Fabry disease.

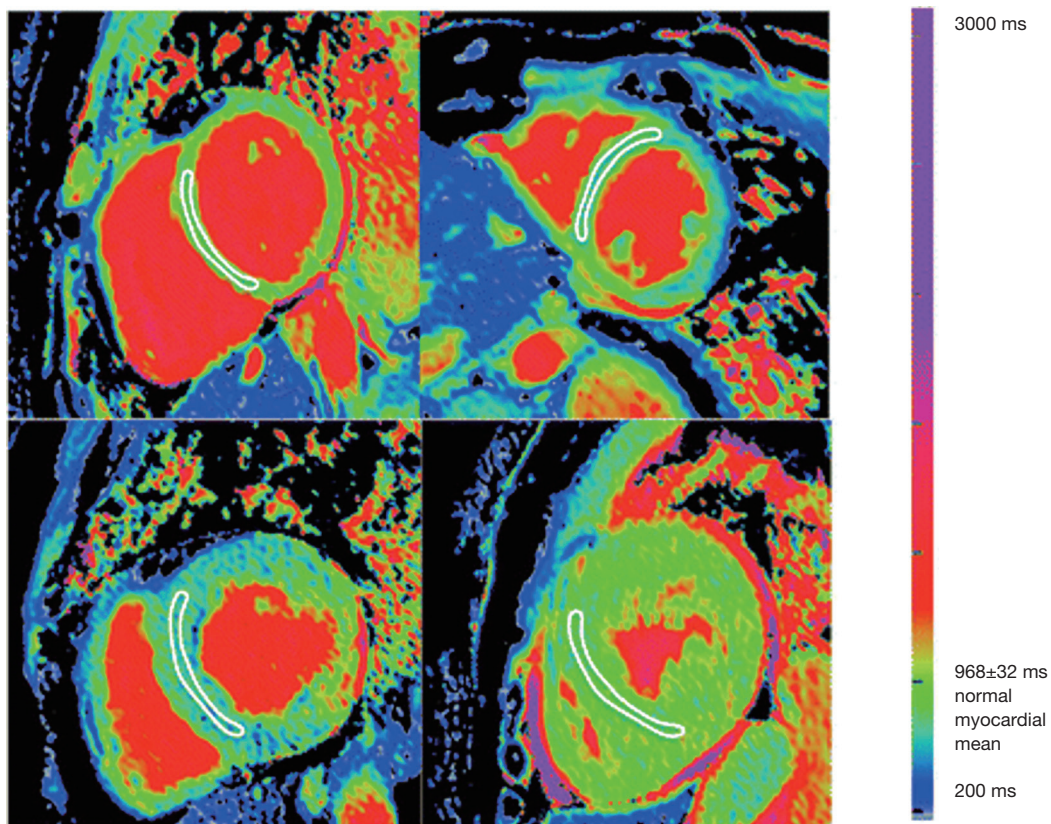


Figure 13 Native T1 mapping in Fabry disease using the ShMOLLI sequence at 1.5 T. Top left: normal. Top right: a Fabry disease subject without LVH but clear myocardial T1 reduction – the myocardium is blue. Bottom left: Typical T1 when LVH present: the myocardial T1 is lower than without LVH and the basal infero-lateral wall has T1 elevation with a normal (pseudonormal?) surrounding area. Bottom right: rarely (4 patients), Fabry disease has a normal T1. Reproduced with without changes under Creative Commons license from Pica *et al.* (33).

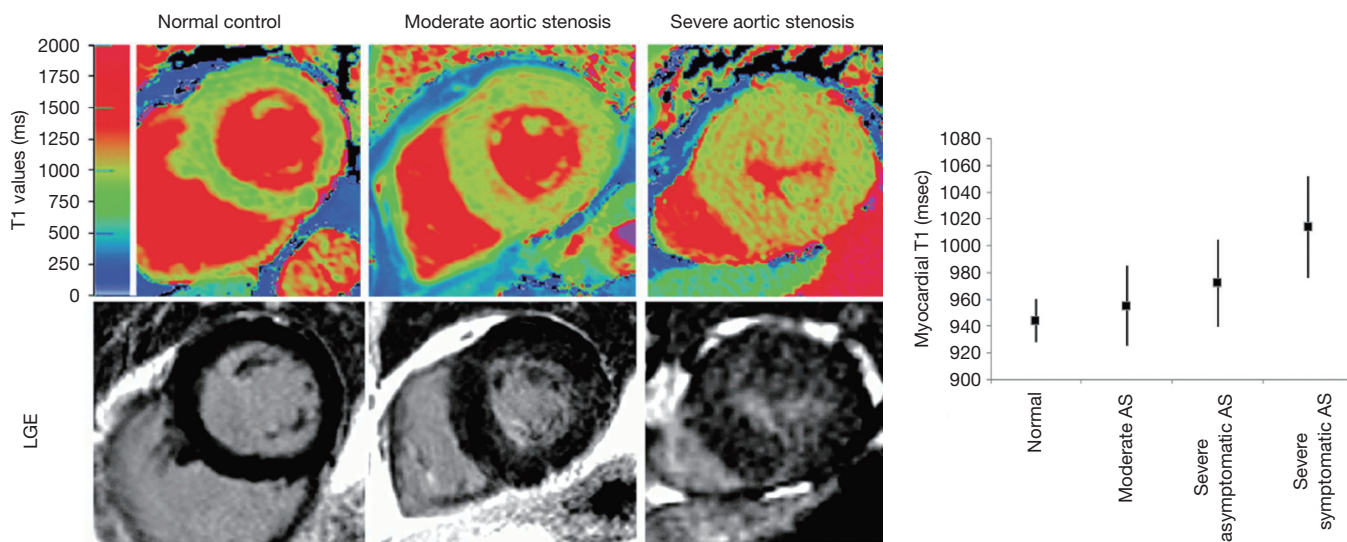


Figure 14 Native T₁ mapping in aortic stenosis. T₁ values of mid-ventricular short-axis slices (top row) and corresponding LGE images (bottom row) of normal controls and patients with moderate and severe AS. The left column shows a normal volunteer (T₁=944 ms), the middle column a patient with moderate AS and moderate left ventricular hypertrophy (T₁=951 ms) and the right column shows a patient with severe AS with severe left ventricular hypertrophy (T₁=1,020 ms). B Whisker-plots of myocardial T₁ values of normal controls and of patients with moderate AS, asymptomatic severe AS and symptomatic severe AS. The between-group comparisons with the corresponding p-values are also presented. AS aortic stenosis, LGE late gadolinium enhancement, ns non-significant. Reproduced and adapted with permission under Creative Commons license from Bull *et al.* (38).

are frequently limited by adverse acoustic windows (36), and athletic heart, where discrimination from HCM is also commonly sought. The assessment of LGE can be valuable as it is more likely to be seen or to have a characteristic pattern reflecting one of the pathological caused outlined above.

Mid-wall enhancement is seen with severe chronic pressure remodelling and is detected in 19–62% of patients with severe AS where it is has prognostic value (37). Again T₁ mapping has been investigated extensively in this arena. Overall, whilst on a group basis, native T₁ mapping techniques can separate out severe aortic stenosis from non-pressure loaded hearts, the overlap is considerable, and the elevation in T₁ itself not specific. Bull and colleagues showed that LV native T₁ values were significantly higher among patients with symptomatic severe AS compared with moderate and asymptomatic severe AS (1,014±38 *vs.* 955±30 and 972±33 ms, respectively at 1.5 T; P<0.05 (Figure 14). A significant correlation was observed between native T₁ values and collagen volume fraction assessed on myocardial biopsies (R=0.65, P=0.002) (38). Post contrast ECV mapping has also been shown to strongly correlated with the histological collagen volume fraction (R²=0.86; P<0.001) in Severe AS (39), and also to be prognostic (40).

Whether CMR has value in guiding early intervention in aortic stenosis is the topic of ongoing clinical studies.

Conclusions

Determination of the underlying aetiology of left ventricular hypertrophy remains a challenging but important clinical problem. Through detailed anatomical imaging, and tissue characterization with LGE, T₁ mapping and DTI the diagnostic arsenal available for the assessment of left ventricular hypertrophy has increased greatly. In the current era, CMR allows a detailed and comprehensive work-up of hypertrophied hearts and can enable the non-invasive and safe diagnosis of the underlying origin in various cardiovascular diseases making it now arguably the gold standard.

Acknowledgments

Funding: None.

Footnote

Provenance and Peer Review: This article was commissioned by

the Guest Editors (Oliver Rider and Andrew J. Lewis) for the series “The use of advanced cardiac MRI in heart failure and cardiac hypertrophy” published in *Cardiovascular Diagnosis and Therapy*. The article was sent for external peer review organized by the Guest Editors and the editorial office.

Conflicts of Interest: All authors have completed the ICMJE uniform disclosure form (available at <http://dx.doi.org/10.21037/cdt.2020.01.14>). The series “The Use of Advanced Cardiac MRI in Heart Failure and Cardiac Hypertrophy” was commissioned by the editorial office without any funding or sponsorship. AJML and OJR served as the unpaid Guest Editors of the series. The authors have no other conflicts of interest to declare.

Ethical Statement: The authors are accountable for all aspects of the work in ensuring that questions related to the accuracy or integrity of any part of the work are appropriately investigated and resolved.

Open Access Statement: This is an Open Access article distributed in accordance with the Creative Commons Attribution-NonCommercial-NoDerivs 4.0 International License (CC BY-NC-ND 4.0), which permits the non-commercial replication and distribution of the article with the strict proviso that no changes or edits are made and the original work is properly cited (including links to both the formal publication through the relevant DOI and the license). See: <https://creativecommons.org/licenses/by-nc-nd/4.0/>.

References

- Rider OJ, Ntusi N, Bull SC, et al. Improvements in ECG accuracy for diagnosis of left ventricular hypertrophy in obesity. *Heart* 2016;102:1566-72.
- Rider OJ, Lewandowski A, Nethononda R, et al. Gender-specific differences in left ventricular remodelling in obesity: insights from cardiovascular magnetic resonance imaging. *Eur Heart J* 2013;34:292-9.
- Authors/Task Force members, Elliott PM, Anastasakis A, et al. 2014 ESC Guidelines on diagnosis and management of hypertrophic cardiomyopathy: the Task Force for the Diagnosis and Management of Hypertrophic Cardiomyopathy of the European Society of Cardiology (ESC). *Eur Heart J* 2014;35:2733-79.
- Gersh BJ, Maron BJ, Bonow RO, et al. 2011 ACCF/AHA Guideline for the Diagnosis and Treatment of Hypertrophic Cardiomyopathy: a report of the American College of Cardiology Foundation/American Heart Association Task Force on Practice Guidelines. Developed in collaboration with the American Association for Thoracic Surgery, American Society of Echocardiography, American Society of Nuclear Cardiology, Heart Failure Society of America, Heart Rhythm Society, Society for Cardiovascular Angiography and Interventions, and Society of Thoracic Surgeons. *J Am Coll Cardiol* 2011;58:e212-60.
- Pinney JH, Whelan CJ, Petrie A, et al. Senile systemic amyloidosis: clinical features at presentation and outcome. *J Am Heart Assoc* 2013;2:e000098.
- Maceira AM, Joshi J, Prasad SK, et al. Cardiovascular magnetic resonance in cardiac amyloidosis. *Circulation* 2005;111:186-93.
- Raina S, Lensing SY, Nairouz RS, et al. Prognostic Value of Late Gadolinium Enhancement CMR in Systemic Amyloidosis. *JACC Cardiovasc Imaging* 2016;9:1267-77.
- Dungu JN, Valencia O, Pinney JH, et al. CMR-based differentiation of AL and ATTR cardiac amyloidosis. *JACC Cardiovasc Imaging* 2014;7:133-42.
- Brownrigg J, Lorenzini M, Lumley M, et al. Diagnostic performance of imaging investigations in detecting and differentiating cardiac amyloidosis: a systematic review and meta-analysis. *ESC Heart Fail* 2019;6:1041-51.
- Di Bella G, Minutoli F, Mazzeo A, et al. MRI of cardiac involvement in transthyretin familial amyloid polyneuropathy. *AJR Am J Roentgenol* 2010;195:W394-9.
- Maurer MS, Schwartz JH, Gundapaneni B, et al. Tafamidis Treatment for Patients with Transthyretin Amyloid Cardiomyopathy. *N Engl J Med* 2018;379:1007-16.
- Adams D, Gonzalez-Duarte A, O’Riordan WD, et al. Patisiran, an RNAi therapeutic, for hereditary transthyretin amyloidosis. *N Engl J Med* 2018;379:11-21.
- Solomon SD, Adams D, Kristen A, et al. Effects of Patisiran, an RNA Interference Therapeutic, on Cardiac Parameters in Patients With Hereditary Transthyretin-Mediated Amyloidosis. *Circulation* 2019;139:431-43.
- Benson MD, Waddington-Cruz M, Berk JL, et al. Inotersen treatment for patients with hereditary transthyretin amyloidosis. *New England Journal of Medicine* 2018;379:22-31.
- Liu JM, Liu A, Leal J, et al. Measurement of myocardial native T1 in cardiovascular diseases and norm in 1291 subjects. *J Cardiovasc Magn Reson* 2017;19:74.
- Banypersad SM, Sado DM, Flett AS, et al. Quantification of myocardial extracellular volume fraction in systemic AL amyloidosis: an equilibrium contrast cardiovascular magnetic resonance study. *Circ Cardiovasc Imaging* 2013;6:34-9.

17. Gati S, Sharma S, Pennell D. The role of cardiovascular magnetic resonance imaging in the assessment of highly trained athletes. *JACC: Cardiovascular Imaging* 2018;11:247-59.
18. Kramer CM, Appelbaum E, Desai MY, et al. Hypertrophic Cardiomyopathy Registry: The rationale and design of an international, observational study of hypertrophic cardiomyopathy. *Am Heart J* 2015;170:223-30.
19. Freitas P, Ferreira AM, Arteaga-Fernandez E, et al. The amount of late gadolinium enhancement outperforms current guideline-recommended criteria in the identification of patients with hypertrophic cardiomyopathy at risk of sudden cardiac death. *J Cardiovasc Magn Reson* 2019;21:50.
20. Hinojar R, Varma N, Child N, et al. T1 Mapping in Discrimination of Hypertrophic Phenotypes: Hypertensive Heart Disease and Hypertrophic Cardiomyopathy: Findings From the International T1 Multicenter Cardiovascular Magnetic Resonance Study. *Circ Cardiovasc Imaging* 2015. doi: 10.1161/CIRCIMAGING.115.003285.
21. Ariga R, Tunnicliffe EM, Manohar SG, et al. Identification of Myocardial Disarray in Patients With Hypertrophic Cardiomyopathy and Ventricular Arrhythmias. *J Am Coll Cardiol* 2019;73:2493-502.
22. Rybicki BA, Major M, Popovich J Jr, et al. Racial differences in sarcoidosis incidence: a 5-year study in a health maintenance organization. *Am J Epidemiol* 1997;145:234-41.
23. Iwai K, Takemura T, Kitaichi M, et al. Pathological studies on sarcoidosis autopsy. II. Early change, mode of progression and death pattern. *Acta Pathol Jpn* 1993;43:377-85.
24. Birnie DH, Sauer WH, Bogun F, et al. HRS expert consensus statement on the diagnosis and management of arrhythmias associated with cardiac sarcoidosis. *Heart Rhythm* 2014;11:1305-23.
25. Patel MR, Cawley PJ, Heitner JF, et al. Detection of myocardial damage in patients with sarcoidosis. *Circulation* 2009;120:1969-77.
26. Puntmann VO, Isted A, Hinojar R, et al. T1 and T2 mapping in recognition of early cardiac involvement in systemic sarcoidosis. *Radiology* 2017;285:63-72.
27. Youssef G, Leung E, Mylonas I, et al. The use of 18F-FDG PET in the diagnosis of cardiac sarcoidosis: a systematic review and metaanalysis including the Ontario experience. *J Nucl Med* 2012;53:241-8.
28. Dweck MR, Abgral R, Trivieri MG, et al. Hybrid Magnetic Resonance Imaging and Positron Emission Tomography With Fluorodeoxyglucose to Diagnose Active Cardiac Sarcoidosis. *JACC Cardiovasc Imaging* 2018;11:94-107.
29. Lewis AJ, Miller JJ, Lau AZ, et al. Noninvasive immunometabolic cardiac inflammation imaging using hyperpolarized magnetic resonance. *Circulation research* 2018;122:1084-93.
30. Miller JJ, Lau AZ, Nielsen PM, et al. Hyperpolarized [1, 4-13C2] fumarate enables magnetic resonance-based imaging of myocardial necrosis. *JACC: Cardiovascular Imaging* 2018;11:1594-606.
31. Wicks EC, Menezes LJ, Barnes A, et al. Diagnostic accuracy and prognostic value of simultaneous hybrid 18F-fluorodeoxyglucose positron emission tomography/magnetic resonance imaging in cardiac sarcoidosis. *Eur Heart J Cardiovasc Imaging* 2018;19:757-67.
32. Deva DP, Hanneman K, Li Q, et al. Cardiovascular magnetic resonance demonstration of the spectrum of morphological phenotypes and patterns of myocardial scarring in Anderson-Fabry disease. *J Cardiovasc Magn Reson* 2016;18:14.
33. Pica S, Sado DM, Maestrini V, et al. Reproducibility of native myocardial T1 mapping in the assessment of Fabry disease and its role in early detection of cardiac involvement by cardiovascular magnetic resonance. *J Cardiovasc Magn Reson* 2014;16:99.
34. Rider OJ, Francis JM, Ali MK, et al. Determinants of left ventricular mass in obesity; a cardiovascular magnetic resonance study. *J Cardiovasc Magn Reson* 2009;11:9.
35. Rider OJ, Lewis AJ, Neubauer S. Structural and metabolic effects of obesity on the myocardium and the aorta. *Obesity facts* 2014;7:329-38.
36. Rider OJ, Nethononda R, Petersen SE, et al. Concentric left ventricular remodeling and aortic stiffness: a comparison of obesity and hypertension. *Int J Cardiol* 2013;167:2989-94.
37. Dweck MR, Joshi S, Murigu T, et al. Midwall fibrosis is an independent predictor of mortality in patients with aortic stenosis. *J Am Coll Cardiol* 2011;58:1271-9.
38. Bull S, White SK, Piechnik SK, et al. Human non-contrast T1 values and correlation with histology in diffuse fibrosis. *Heart* 2013;99:932-7.
39. Flett AS, Hayward MP, Ashworth MT, et al. Equilibrium contrast cardiovascular magnetic resonance for the measurement of diffuse myocardial fibrosis: preliminary validation in humans. *Circulation* 2010;122:138-44.
40. Chin CWL, Everett RJ, Kwiecinski J, et al. Myocardial Fibrosis and Cardiac Decompensation in Aortic Stenosis. *JACC Cardiovasc Imaging* 2017;10:1320-33.

Cite this article as: Lewis AJM, Rider OJ. The use of cardiovascular magnetic resonance for the assessment of left ventricular hypertrophy. *Cardiovasc Diagn Ther* 2020;10(3):568-582. doi: 10.21037/cdt.2020.01.14